ORIGINAL ARTICLE

Energy-sparing by 2-methyl-2-thiazoline protects heart from ischaemia/reperfusion injury

Masahiro Nishi[1,2], Takehiro Ogata[3]* 🆔, Ko Kobayakawa[4], Reiko Kobayakawa[4], Tomohiko Matsuo[4], Carlo Vittorio Cannistraci[5,6], Shinya Tomita[1], Shunta Taminishi[1], Takaomi Suga[1], Tomoya Kitani[1], Yusuke Higuchi[1], Akira Sakamoto[1], Yumika Tsuji[1], Tomoyoshi Soga[7] and Satoaki Matoba[1]

[1]Department of Cardiovascular Medicine, Graduate School of Medical Science, Kyoto Prefectural University of Medicine, Kyoto, Japan; [2]Cardiovascular Branch, National Heart, Lung and Blood Institute, National Institutes of Health, Bethesda, MD, USA; [3]Department of Pathology and Cell Regulation, Graduate School of Medical Science, Kyoto Prefectural University of Medicine, Kyoto, 602-8566, Japan; [4]Functional Neuroscience Lab, Kansai Medical University, Hirakata, Japan; [5]Center for Complex Network Intelligence (CCNI), Tsinghua Laboratory of Brain and Intelligence (THBI), Department of Computer Science, Department of Biomedical Engineering, Tsinghua University, China; [6]Center for Systems Biology Dresden (CSBD), Dresden, Germany; and [7]Institute for Advanced Biosciences, Keio University, Tsuruoka, Japan

Abstract

Aims   Cardiac ischaemia/reperfusion (I/R) injury remains a critical issue in the therapeutic management of ischaemic heart failure. Although mild hypothermia has a protective effect on cardiac I/R injury, more rapid and safe methods that can obtain similar results to hypothermia therapy are required. 2-Methyl-2-thiazoline (2MT), an innate fear inducer, causes mild hypothermia resulting in resistance to critical hypoxia in cutaneous or cerebral I/R injury. The aim of this study is to demonstrate the protective effect of systemically administered 2MT on cardiac I/R injury and to elucidate the mechanism underlying this effect.

Methods and results   A single subcutaneous injection of 2MT (50 mg/kg) was given prior to reperfusion of the I/R injured 10 week-old male mouse heart and its efficacy was evaluated 24 h after the ligation of the left anterior descending coronary artery. 2MT preserved left ventricular systolic function following I/R injury (ejection fraction, %: control 37.9 ± 6.7, 2MT 54.1 ± 6.4, $P < 0.01$). 2MT also decreased infarct size (infarct size/ischaemic area at risk, %: control 48.3 ± 12.1, 2MT 25.6 ± 4.2, $P < 0.05$) and serum cardiac troponin levels (ng/mL: control 8.9 ± 1.1, 2MT 1.9 ± 0.1, $P < 0.01$) after I/R. Moreover, 2MT reduced the oxidative stress-exposed area within the heart (%: control 25.3 ± 4.7, 2MT 10.8 ± 1.4, $P < 0.01$). These results were supported by microarray analysis of the mouse hearts. 2MT induced a transient, mild decrease in core body temperature (°C: −2.4 ± 1.4), which gradually recovered over several hours. Metabolome analysis of the mouse hearts suggested that 2MT minimized energy metabolism towards suppressing oxidative stress. Furthermore, 18F-fluorodeoxyglucose-positron emission tomography/computed tomography imaging revealed that 2MT reduced the activity of brown adipose tissue (standardized uptake value: control 24.3 ± 6.4, 2MT 18.4 ± 5.8, $P < 0.05$). 2MT also inhibited mitochondrial respiration and glycolysis in rat cardiomyoblasts.

Conclusions   We identified the cardioprotective effect of systemically administered 2MT on cardiac I/R injury by sparing energy metabolism with reversible hypothermia. Our results highlight the potential of drug-induced hypothermia therapy as an adjunct to coronary intervention in severe ischaemic heart disease.

Introduction

Ischaemic heart disease continues to be the highest cause of mortality worldwide and presents a tremendous burden on society.[1] Notably, myocardial infarction (MI) followed by heart failure demonstrates high morbidity and mortality. Early revascularization by thrombolytic therapy and coronary intervention, along with established emergency cardiac care systems, has improved the prognosis of MI despite the increased morbidity.[2–4] However, patients with a severe MI grade continue to present a poor prognosis.[5] Coronary ischaemia/reperfusion (I/R) injury is still considered a critical issue in the therapeutic management of ischaemic heart failure. Mitochondrial respiration produces oxidative stress causing myocardial I/R injury.[6,7] Although various clinical trials have been launched to improve the treatment of coronary I/R injury, most have failed to reveal effective results except for ischaemic preconditioning and hypothermia therapy.[8]

Accumulating evidence has revealed that hypothermia therapy has a cardioprotective effect. Several studies have demonstrated the cardioprotective effect of hypothermia in mice and pigs.[9,10] In addition to animal studies, previous clinical trials, RAPID-MI and CHILL MI studies, have revealed that cooling treatment before percutaneous coronary intervention (PCI) for ST elevated MI (STEMI) is a safe and effective method to reduce infarct size. Hypothermia therapy has been shown to be extremely useful in early revascularization.[11,12] Furthermore, mild hypothermia therapy reduces brain damage by reducing the oxygen demand, reactive oxygen species (ROS) production, and mitochondrial oxidative stress in patients who survive cardiopulmonary arrest.[13,14] Conversely, several studies have reported conflicting results following the application of hypothermia as an adjunct to PCI in patients with STEMI.[15,16] Hypothermia therapy has been associated with an increased frequency of intensive care and delayed commencement of coronary interventions. Therefore, the effects of hypothermia in patients with MI remain controversial, and further trials using a more rapid and feasible treatment are required.

Humans and other animals have intrinsic defensive behaviours related to survival. Fear, a principal emotion, evokes defensive behaviours for survival during hazardous situations.[17–19] In rodents, certain odours elicit innate fear and systemic defensive behaviour. 2,4,5-trimethyl-3-thiazoline (TMT), a fox secretion, and a potent analogue of TMT, 2-methyl-2-thiazoline (2MT), elicit a highly robust freezing response in mice and have been used as an experimental fear odorant.[20] A large-scale genetics screening has revealed that transient receptor potential ankyrin 1 (TRPA1) is involved in the systemic defensive behaviour evoked by predator odour (2MT and TMT).[21] In addition, 2MT evokes physiological responses, as well as defensive behaviours for survival. 2MT has demonstrated resistance to critical hypoxia in cutaneous or cerebral I/R injury following hypothermia.[22] However, mechanisms underlying the systemic effect of 2MT on tissue metabolism and its potential biomedical implications in cardiovascular diseases remain unknown.

Herein, we revealed the cardioprotective effect following subcutaneous 2MT administration by sparing energy metabolism with reversible hypothermia using a mouse model of cardiac I/R injury. The drug-induced hypothermia and optimized metabolism may be able to clarify the optimal therapeutic strategy for severe ischaemic heart disease.

Methods

Detailed methods of the metabolome, intracellular flux, microarray analyses, dihydroethidium (DHE) staining, and measurement of intracellular ROS generation, and mitochondrial superoxide levels are available in the Supporting information.

Mouse model of cardiac ischaemia/reperfusion injury

A mouse model of cardiac I/R injury was established as previously described, with slight modifications.[23] In 10 week-old C57BL/6 background male mice, the left anterior descending coronary arteries were ligated under 1.0% isoflurane anaesthesia for 30 min before reperfusion. The mice were either subcutaneously administered 50 mg/kg of 2MT (Tokyo Chemical Industry Co.) or saline (100 μL) 10 min prior to reperfusion. The rectal temperature was monitored during the procedure and the temperature was maintained using a heating pad before administration. All animal protocols conformed with the Guide for the Care and Use of Laboratory Animals published by the US National Institutes of Health (NIH; Publication no. 85-23, revised 1996) and were approved by the institutional animal care and use committee of the Kyoto Prefectural University of Medicine.

Echocardiography of mouse heart and evaluation of infarct size

To evaluate the acute and chronic effect of 2MT on I/R-injured heart, echocardiography and subsequent experiments were performed 24 h or 3 weeks after ischaemia. Echocardiography was performed using a Vevo 2100 system (VisualSonics) equipped with a 30 MHz microprobe under isoflurane anaesthesia. A blood sample was collected from the left intraventricular chamber using a 26 G syringe needle 24 h after ligation and maintained at room temperature for 2 h. The serum was separated by centrifugation at $1200 \times g$

for 15 min and stored at −80°C. The serum cardiac troponin I level was measured using a high-sensitivity mouse cardiac troponin I enzyme-linked immunosorbent assay (ELISA) kit (Life Diagnostics), according to the manufacturer's instructions. Triphenyltetrazolium chloride (TTC) staining was performed 24 h after ischaemia as previously described with slight modifications.[24] To determine the area at risk, 10% Evans blue dye (0.5 g/kg) was injected into the retro-orbital venous sinus after ligation of the left anterior descending coronary artery. The heart was excised and stored at −80°C. Cross-sections of the heart (1 mm) were immersed in 1.0% TTC in 0.9% saline at 24°C for 2 to 3 min. Then, the vial was continuously agitated in a water bath at 37°C for 15 min, and cross-sections were fixed in 10% neutral buffered formalin for 60 min. Sections were digitally photographed using a Leica MC120 HD microscope camera (Leica Microsystems). Masson's trichrome staining was performed to analyse the fibrotic area 3 weeks after I/R. The fibrotic area, infarct size, and area at risk were quantified using the ImageJ 1.49 software (NIH).

N^ϵ-(hexanonyl) lysine staining of mice hearts

Briefly, the mouse hearts were exposed to 30 min of ischaemia, followed by 60 min of reperfusion. 2MT (50 mg/kg) or saline (100 μL) was subcutaneously administered 10 min before reperfusion. The hearts were collected, rinsed with cold phosphate-buffered saline, cut into 3 mm slices, and then fixed in 4% paraformaldehyde for 20 h. N^ϵ-(hexanonyl) lysine (HEL) staining of mouse hearts was performed using an anti-HEL monoclonal antibody (JaICA), according to the manufacturer's instructions.

Measurement of 2MT concentration in mice tissues

Briefly, mice hearts were excised 30, 60, and 480 min after subcutaneously administering 2MT (50 mg/kg) or saline, and then frozen in liquid nitrogen. The frozen heart tissue was plunged into methanol and homogenized, and heart extracts were prepared after centrifugation. Blood was collected from the left intraventricular chamber in a tube containing 0.1% EDTA. The plasma was separated by centrifugation at 1200 × *g* for 20 min and stored at −80°C. The plasma was plunged into methanol and prepared after centrifugation. Gas chromatography–mass spectrometry (GCMS)-QP2010Ultra (Shimadzu) was used to measure the 2MT concentration. Spline interpolation of the data was performed using GraphPad Prism ver. 8 (GraphPad Software, Inc., La Jolla, CA, USA).

Temperature measurement and telemetry system

FLIR i3 (FLIR) was used to monitor the mouse body temperature. After subcutaneously administering 2MT (50 mg/kg) or saline to 10 week-old C57BL/6 background male mice, the body temperature was continuously monitored under 1.0% isoflurane anaesthesia for 80 min. Physio Tel Digital telemetry platform (DSI) was used to measure the mouse core temperature and heart rate. Based on the surgical procedure described by the manufacturer, an ETA-F10 transmitter was implanted into the abdominal cavity of each mouse. After surgery, the mice were allowed to recover for 7 days. Core temperature and heart rate were measured by the telemetry platform every 10 min after subcutaneously administering 2MT or saline for 12 h.

Peripheral blood flow assay

OZ1 (Omegawave) was used to analyse the peripheral blood flow in mice. After subcutaneously administering 2MT (50 mg/kg) or saline to 10 week-old C57BL/6 background male mice, blood flow in the left hind paw was measured every 5 min for 80 min under 1.0% isoflurane anaesthesia.

Blood glucose, insulin, and glucagon assays

Briefly, 2MT (50 mg/kg) or saline was subcutaneously administered to 10 week-old C57BL/6 background male mice, fasted overnight with free access to water. The blood glucose concentration was measured 30, 60, 120, 240, and 420 min after the 2MT injection. Blood was collected from the left intraventricular chamber in a tube and maintained at room temperature for 2 h. The serum was separated by centrifugation at 1200 × *g* for 15 min and stored at −80°C. Insulin and glucagon concentrations were estimated using Ultra-Sensitive Mouse/Rat Insulin ELISA Kit (Morinaga Institute of Biological Science) and YKO91 Glucagon-HS ELISA kit (Yanaihara Institute Inc), respectively, according to the manufacturer's instructions.

18F-fluorodeoxyglucose-positron emission tomography/computed tomography imaging

Briefly, 10-week-old C57BL/6 background male mice, fasted overnight with free access to water, were subjected to cold exposure for 5 h before imaging. Then, 2MT or saline was subcutaneously administered, and 200 μCi 18F-fluorodeoxyglucose (FDG) was injected via the tail vein 2 h and 1 h before imaging, respectively. Positron emission tomography/computed tomography imaging (PET/CT) was

performed by HITS-655 K (Hamamatsu Photonics KK) with FX Pre-Clinical Platform (GAMMA MEDICA IDEAS). After imaging reconstruction, AMIDE 0.9.0 (Amide's a Medical Imaging Data Examiner) was used to analyse the standardized uptake value (SUV) in regions of interest to quantify the brown adipose tissue (BAT) activity.

Cell culture and extracellular metabolic-flux assay

Briefly, H9C2 cells were cultured using Dulbecco's Modified Eagle Medium (DMEM) containing 10% foetal bovine serum (FBS). Propidium iodide-based cell viability test was performed following 2MT 0, 0.1, 1, 2, 5, or 10 mM treatment for 2 h by ADAM MC Auto Cell Counter (Digital Bio). Seahorse XFe96 Flux Analyser (Agilent) was used to evaluate mitochondrial respiration and glycolysis in the live cells. The cells were seeded on XF 96 microplates and treated with 2MT (0, 0.1, or 1 mM) before measurement. After baseline measurements, oligomycin (1 μM), carbonyl cyanide-p-trifluoromethoxyphenylhydrazone (FCCP, 1 μM), and rotenone/antimycin A (0.5 μM) were sequentially added to each well, and the extracellular acidification rate (ECAR) and oxygen consumption rate (OCR) were measured. For glycolysis stress test, ECAR was measured in H9C2 cells following sequential addition of 2MT (0, 0.1, or 1 mM), glucose (10 mM), oligomycin (1 μM), and 2-deoxy-D-glucose (50 mM). For palmitate oxidation stress test, OCR was measured in H9C2 cells following sequential addition of 2MT (0 or 1 mM), 1 mM palmitate conjugated with 0.17 mM BSA, etomoxir (4 μM), oligomycin (1.5 μM), FCCP (1 μM), and rotenone/antimycin A (0.5 μM).

Western blot analysis

Cell lysates were extracted using a lysis buffer (50 mmol/L Tris–HCl [pH 7.5], 150 mmol/L NaCl, 50 nmol/L EDTA, 1% Triton X-100. Protein samples were subjected to SDS-PAGE and then transferred to membranes that were subsequently incubated with antibody against TRPA1.

Statistical analysis

In the present study, R 3.3.2 (R Foundation for Statistical Computing) was used for statistical analysis.[25] The Shapiro–Wilk test was used for normality testing. All two-group analysis was performed using a two-tailed Student t test. Comparisons of multiple groups were performed with one-way ANOVA, followed by the Tukey *post hoc* test. All data are presented as mean ± standard deviation (SD). All *in vitro* experiments were performed at least three times.

Results

2MT preserves left ventricular systolic function and decreases infarct size in the heart after I/R injury with ameliorated oxidative stress.

To assess whether 2MT has cardioprotective effects in cardiac I/R injury, adult mouse hearts were exposed to ischaemia by ligating the left anterior descending artery for 30 min, followed by reperfusion. The mice were administered 2MT (50 mg/kg) or saline 10 min before reperfusion (*Figure 1A*). Echocardiography was performed to assess the cardiac function after I/R and revealed that 2MT preserved the left ventricular systolic function (ejection fraction, %: control 37.9 ± 6.7, 2MT 54.1 ± 6.4, $P < 0.01$; fraction shortening, %: control 18.1 ± 3.5, 2MT 27.3 ± 4.1, $P < 0.01$) (*Figure 1B*). The infarct size was evaluated by triphenyltetrazolium chloride (TTC) and Evans blue staining. 2MT decreased the infarct size after I/R (infarct size/ischaemic area at risk, %: control 48.3 ± 12.1, 2MT 25.6 ± 4.2, $P < 0.05$) (*Figure 1C* and *1D*). In mice, the serum cardiac troponin I level was significantly reduced by 2MT when compared with the control after cardiac I/R (ng/mL: control 8.9 ± 1.1, 2MT 1.9 ± 0.1, $P < 0.01$) (*Figure 1E*). HEL staining of mouse hearts showed that 2MT reduced the area subjected to oxidative stress in the heart after I/R (HEL positive area, %: I/R-control 25.3 ± 4.7, I/R-2MT 10.8 ± 1.4, $P < 0.01$) (*Figure 2A*). In DHE staining, the intensity of ROS production in I/R-injured heart was reduced by 2MT treatment (ROS intensity: I/R-control 2.7 ± 0.8, I/R-2MT 1.7 ± 0.1, $P < 0.01$) (*Figure S1A*). About H_2O_2-associated ROS generation in H9C2 cells, 2MT reduced, although not significantly, intracellular and mitochondrial ROS generation (intracellular ROS: H_2O_2-control 1.36 ± 0.54, H_2O_2-2MT 1.17 ± 0.47, $P = 0.45$, mitochondrial superoxide: H_2O_2-control 1.25 ± 0.38, H_2O_2-2MT 1.22 ± 0.31, P = 0.35) (*Figure S1B*, *S1C*). We furthermore evaluated the chronic effect of 2MT on the heart. The cardiac function was preserved, and the fibrotic area was decreased 3 weeks after a subcutaneous 2MT injection (*Figure S2*).

The mouse left ventricles underwent microarray analysis 4 h after the 2MT injection. Considering that the phenotypic change of heart function occurred at 24 h after ischaemia, we set earlier time point for microarray analysis. A heat map of differential gene expression was exhibited (*Figure 2B*). Principal component analysis (PCA) showed a distinctive separation between the 2MT (n = 3) and control (n = 3) groups in the direction of PC1 (*Figure 2C*). PC1 loading of each gene and their correlation coefficients were used to build the PC-corr network, which represents the association between the discriminative genes associated with the 2MT perturbation (*Figure S3*). For genes in the PC-corr network, pathway enrichment analysis presented the response to oxidative stress, and the regulation of cell death was significantly associated with the cardiac effect of 2MT (*Figure 2D*). Nonetheless, the volcano plot of the microarray did not indicate

Figure 1 2MT preserves left ventricular systolic function and reduces infarct size in the heart after ischaemia/reperfusion injury. (A) Schematic outline of study workflow. A mouse model of cardiac I/R injury was established. In 10 week-old male mice, the left anterior descending coronary arteries were ligated for 30 min before reperfusion. 2MT (50 mg/kg) or saline was subcutaneously injected to the mice 10 min before reperfusion. Hearts were analysed 24 h after ligation. (B) FS and EF were assessed by echocardiography for sham or I/R operated mice after saline or 2MT injection (*n* = 7 for each group). Representative images after Evans blue injection and subsequent TTC staining (C) and quantification of the area at risk (left graph) and infarct size (right graph) (D) (*n* = 4 for each group). (E) Serum cardiac troponin I level in I/R operated mice after saline or 2MT injection (control *n* = 5, 2MT *n* = 4). *P < 0.05, **P < 0.01; one-way ANOVA with Tukey *post hoc* test for multiple group analysis and two-tailed Student *t* test for two-group analysis. All values are mean ± standard deviation (SD). Each dot represents one mouse. 2MT, 2-methyl-2-thiazoline; AAR, area at risk; EF, ejection fraction; FS, fraction shortening; I/R, ischaemia–reperfusion; IS, infarct size; LV, left ventricle; s.c., subcutaneous administration; TTC, triphenyltetrazolium chloride.
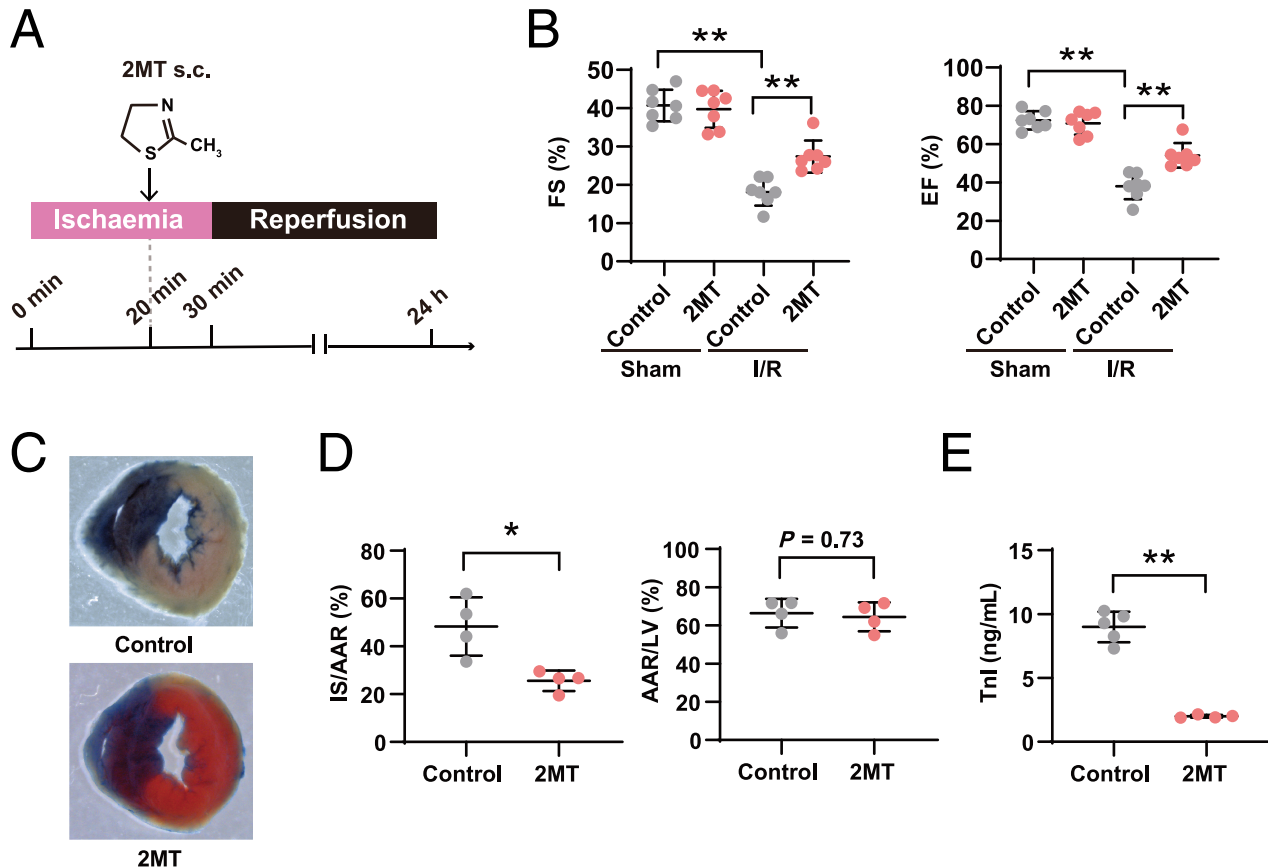

the specific impactful target gene of 2MT in terms of the cardioprotective mechanism (*Figure S4*). Further, microarray analysis for I/R-injured mice heart showed that 2MT is likely to be associated with the regulation of inflammation including cytokine and interleukin-1, and skeletal muscle cell differentiation (*Figure S5*). Collectively, a single subcutaneous injection of 2MT induced a response that protected against cardiac damage induced by I/R injury via these specific pathways.

Systemic distribution of 2MT temporarily declines core temperature

To evaluate the physiological response to 2MT, the surface and core temperatures of the mice were measured after subcutaneously administering 2MT. A thermal imaging camera showed that the body temperature declined after subcutaneously administering 2MT (*Figure 3A*). Additionally, the core temperature was mildly and temporarily reduced (°C: −2.4 ± 1.4) following the administration of 2MT at 50 mg/kg and recovered gradually over 8 h (*Figure 3B*), whereas 2MT at 100 mg/kg showed the prolonged and extreme decline of core temperature (*Figure S6*). The heart rate measured using a telemetry system did not differ between the 2MT and control groups (*Figure 3C*). To reveal tissue distribution in subcutaneously injected-2MT mice, the 2MT concentration was measured in the heart and plasma. The cubic spline curve analysis showed that the 2MT concentration could be detected in the plasma and heart after subcutaneous administration (*Figure 3D*). Peripheral blood

Figure 2 2MT ameliorates oxidative stress in the heart after ischaemia/reperfusion. (A) Representative images of HEL staining of mice hearts 1 h after sham or I/R operation, followed by saline or 2MT injection, and its quantification (n = 5 for each group). The scale bar indicates 50 μm. **$P < 0.01$; two-tailed Student t test. (B) Heat map of differential gene expression. (C) Principal component analysis of microarray data (n = 3 for each group). Red nodes indicate 2MT; black nodes indicate control. (D) Enrichment analysis conducted by DAVID. The top 10 GO pathways are ranked by Benjamini-adjusted P values and scaled according to the function-log10 (P value). 2MT, 2-methyl-2-thiazoline; HEL, N^{ε}-(hexanonyl) lysine; I/R, ischaemia–reperfusion; PC1, first principal component; PC2, second principal component.
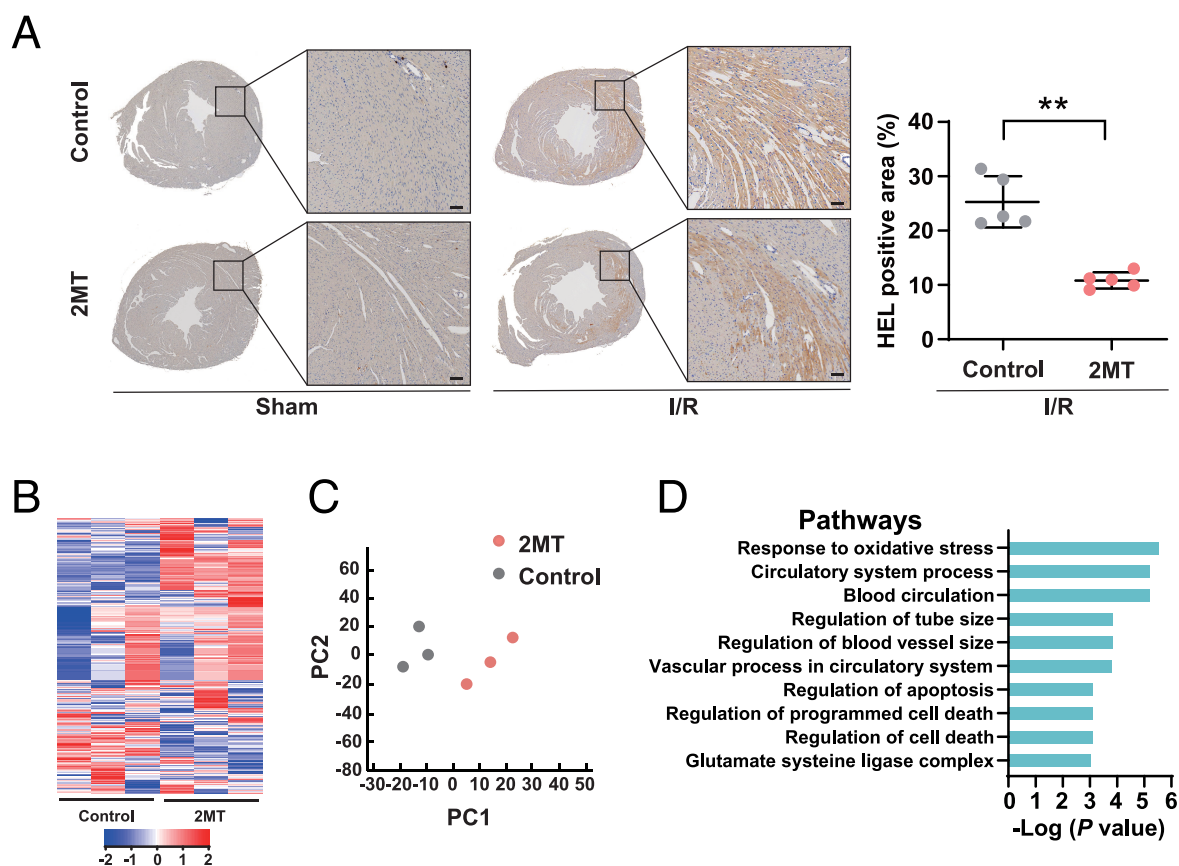

flow controls the body temperature through heat emission, and we measured the blood flow in the mouse hind paw. Following 2MT administration, the peripheral blood flow was reduced then followed by recovery, which can be explained as a physiological response to cold exposure in mammals (*Figure 3E* and *3F*). These results revealed that subcutaneously injected-2MT was systemically distributed and temporarily reduced core temperature.

2MT optimally modulates energy metabolism in the mouse heart

To validate whether 2MT affects metabolic changes in the heart, a metabolome analysis was performed on mouse hearts after a subcutaneous 2MT injection. Mouse hearts were excised 0, 30, 240, and 480 min after the injection to a cover broad time range. PCA (8 control vs. 12 2MT) showed a separation between the 2MT and control groups

(*Figure 4A*). The PC1 loading of each metabolite and their correlation coefficients were used to build the PC-corr network (*Figure 4B*), representing the association between discriminative metabolites following 2MT administration. Enrichment analysis of the metabolites in the PC-corr network showed that several metabolic pathways are associated with 2MT. Among these, energy metabolism pathways such as glycolysis, oxidative phosphorylation, and the tricarboxylic acid (TCA) cycle were enriched (*Figure 4C*). Regarding metabolites of glycolysis, 2MT reduced dihydroxyacetone phosphate (DHAP) but not glucose-1-phosphate (G1P) (*Figure 5A*). Anaerobic respiration was not activated as 2MT reduced the lactate content. Furthermore, 2MT decreased metabolites of the TCA cycle and oxidative phosphorylation. Fumarate, a metabolite of the TCA cycle, was reduced by 2MT, although citrate and malate were unchanged (*Figure 5B*). Additionally, 2MT increased acetyl-CoA. Notably, 2MT increased a cofactor for redox signalling, that is, nicotinamide adenine dinucleotide (NADH), known to increase during energy overload.[1,26]

Figure 3 Systemic distribution of 2MT declines core temperature. (A) Images captured by mice thermography, before and 1 h after a subcutaneous injection of saline (left mouse) or 2MT (50 mg/kg; right mouse). (B) Mice core temperature measured using a telemetry system after a subcutaneous injection of 2MT (50 mg/kg) or saline (left graph) and changes 1 h after the 2MT injection (right graph) (*n* = 7 for each group). (C) The heart rate was measured using the telemetry system after a subcutaneous injection of 2MT (50 mg/kg) or saline (*n* = 5 for each group). (D) Concentration of 2MT in mouse plasma and heart measured by GCMS (*n* = 4 for each group). The magenta line indicates plasma; the cyan line indicates heart. The left *Y*-axis indicates the plasma concentration; the right *Y*-axis indicates concentration in the heart. (E and F) Peripheral blood flow in mice after a subcutaneous injection of 2MT (50 mg/kg) or saline. Representative images before and 10 min after the 2MT injection (E), its quantification (left graph), and changes (right graph) (F) (*n* = 6 for each group). *$P < 0.05$, **$P < 0.01$; two-tailed Student *t* test. All values are mean ± standard deviation (SD). Each dot represents one mouse. 2MT, 2-methyl-2-thiazoline; GCMS, gas chromatography–mass spectrometry.
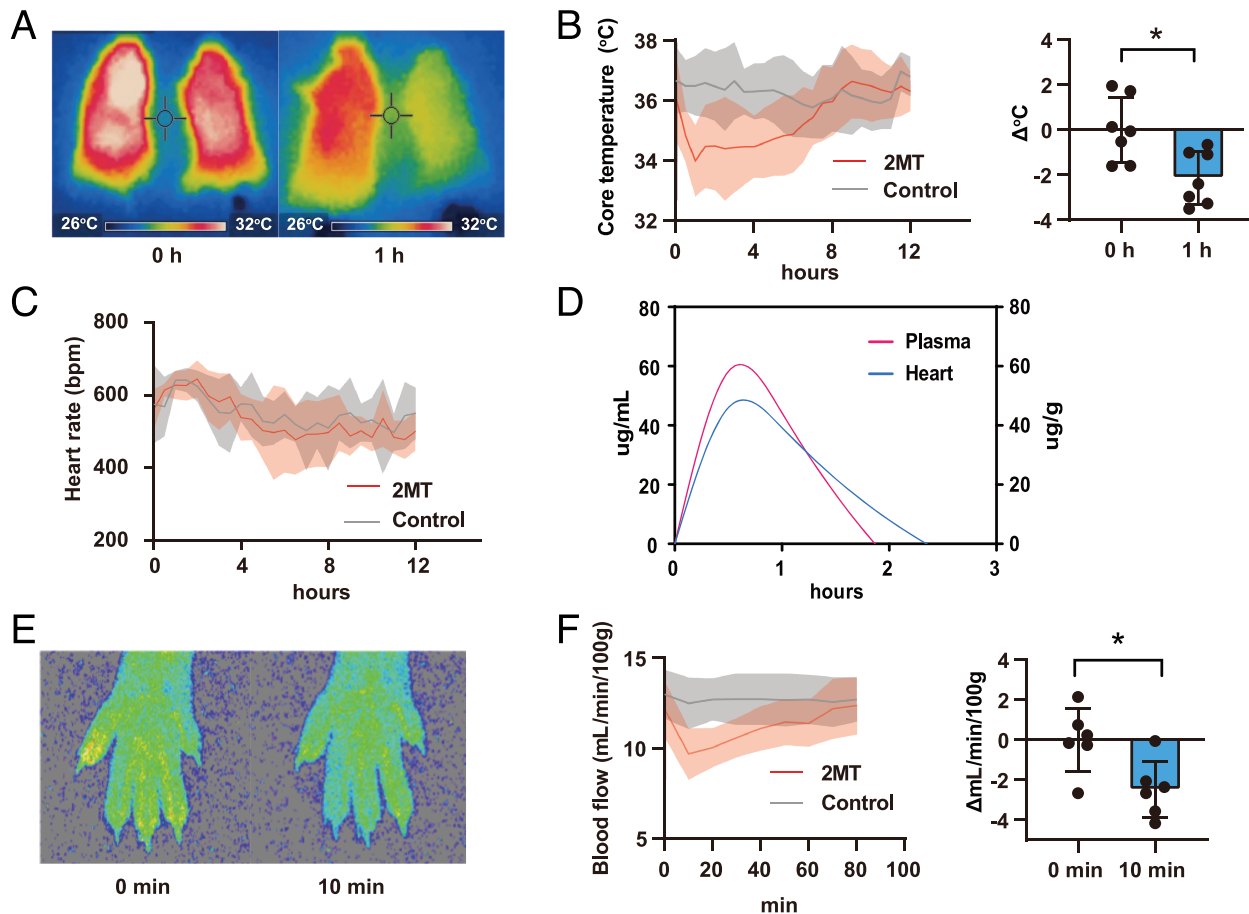

No significant change was observed in the amount of ATP, but the administration of 2MT demonstrated a significant increase in ADP levels (*Figure 5B*). This imbalance between ADP and ATP suggested that 2MT abruptly suppressed the efficiency of ADP-to-ATP production via cellular respiration. Adenylate energy charge, an indicator that reflects the state of total energy conservation in cardiac tissue,[27,28] was not significantly different but tended to increase after 2MT administration (*Figure S7*). To assess intracellular metabolic glucose alterations, an intracellular flux analysis was performed after intraperitoneally administering 13C glucose to 2MT or saline-administered mouse hearts. Mouse hearts were excised 30 min after 2MT injection to investigate the rapid reaction of glucose metabolism. Unexpectedly, 2MT failed to decrease the proportion of glycolysis-related metab-

olites; however, metabolites of the TCA cycle were reduced when compared with the control. This is consistent with the results of the metabolome analysis (*Figure S8*). 2MT relatively reduced succinate levels when compared with the control. The reduced succinate levels may clarify the mechanism through which 2MT demonstrates a protective effect on the ischaemic heart. These results indicated that 2MT optimally modulates energy metabolism in the mouse heart.

2MT modulates energy metabolism by inhibition of glycolysis and mitochondrial respiration

To further investigate the impact of 2MT on glucose metabolism, blood glucose levels were measured following the

Figure 4 Network analysis reveals the association of discriminative metabolites following 2MT administration. (A) Principal component analysis of metabolome data after a subcutaneous injection of 2MT (50 mg/kg) or saline. Red nodes indicate 2MT; black nodes indicate control. (B) PC-corr network between metabolites constructed with a cutoff of 0.6. Perturbed metabolites are depicted according to the size and colour shading of nodes. Black and red colours indicate up-regulated perturbation in control and 2MT, respectively. (C) Enrichment analysis conducted by MBROLE. The top 12 pathways are ranked by Benjamini-adjusted P values and scaled according to the function-log10 (P value). 2MT, 2-methyl-2-thiazoline; PC1, first principal component; PC2, second principal component.
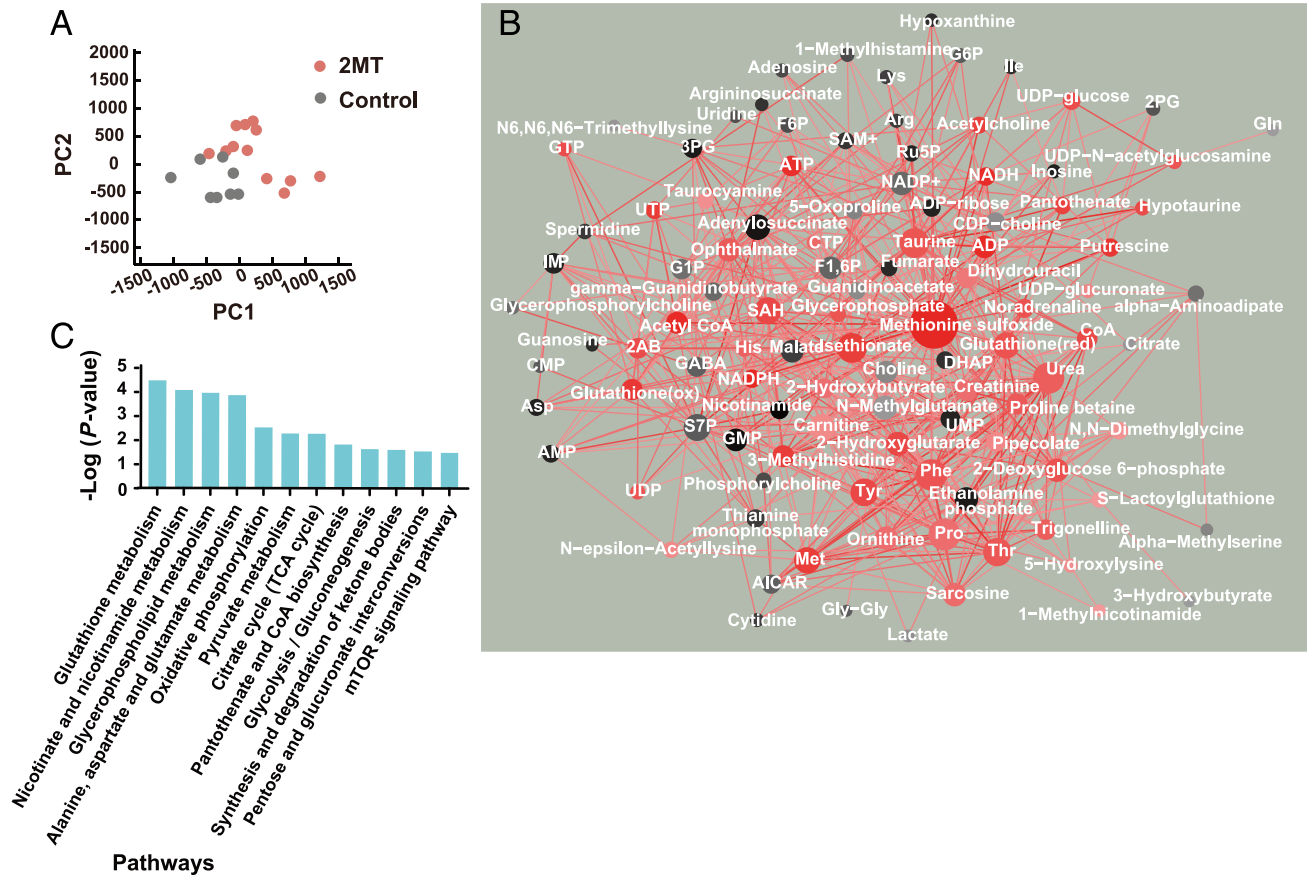

subcutaneous administration of 2MT or saline in mice. Compared with saline controls, 2MT increased blood glucose levels (*Figure 6A*). The blood insulin level was increased, although the blood glucagon level was unchanged by 2MT (*Figure 6B*). These results indicated that 2MT inhibits glucose uptake in mouse tissues. Next, we performed fluorodeoxyglucose-positron emission tomography/computed tomography (FDG PET/CT) imaging to assess brown adipose tissue (BAT) activation in mice after a subcutaneous injection of 2MT or saline. Cold exposure was necessary for the BAT activation to be detected by PET-CT. Because the hypothermic effect of 2MT was maximal for 1 to 2 h after administration, 2MT was administered 2 h before imaging to investigate the glucose metabolism-related BAT activation. BAT is considered a central organ where energy expenditure and heat production are conducted with uncoupling protein 1 (UCP1) activation. The uptake of 18F-fluorodeoxyglucose

(18F-FDG) detected by PET/CT is a metabolic activity indicator of BAT in mammals, including humans.[29,30] In mice administered with 2MT, the SUV of BAT was lower than that in control mice after 4°C cold exposure (SUV: control 24.3 ± 6.4, 2MT 18.4 ± 5.8, $P < 0.05$) (*Figure 6C*). Decreased glucose uptake following 2MT administration might induce the inactivation of BAT, which can partially contribute to the 2MT-induced temperature decrease. The uptake of 18F-FDG into the heart was not able to be precisely detected because the signal of BAT was much stronger than other adjacent tissue. Rat cardiomyoblasts, H9C2 cells, were used to evaluate the mitochondrial respiratory function. We performed a cell viability test for H9C2 cells following 2MT treatment for 2 h. As a result, the cells were viable with the treatment of 2MT 0.1–5 mM, but 10 mM showed toxicity to the cells (*Figure S9*). We performed a western blot analysis of TRPA1 in rat cardiomyocyte and H9C2 cells. Consequently, we

Figure 5 2MT optimally modulates energy metabolism in the heart. Quantification of metabolites involved in glycolysis (A), the TCA cycle, and oxidative phosphorylation (B). *n* = 8 and 12 in control and 2MT-treated group respectively except for DHAP, *n* = 7 and 9. *P < 0.05, **P < 0.01; two-tailed Student *t* test. All values are mean ± standard deviation (SD). Each dot represents one mouse. 2MT, 2-methyl-2-thiazoline; DHAP, dihydroxyacetone phosphate; G1P, glucose-1-phosphate; NADH, nicotinamide adenine dinucleotide.
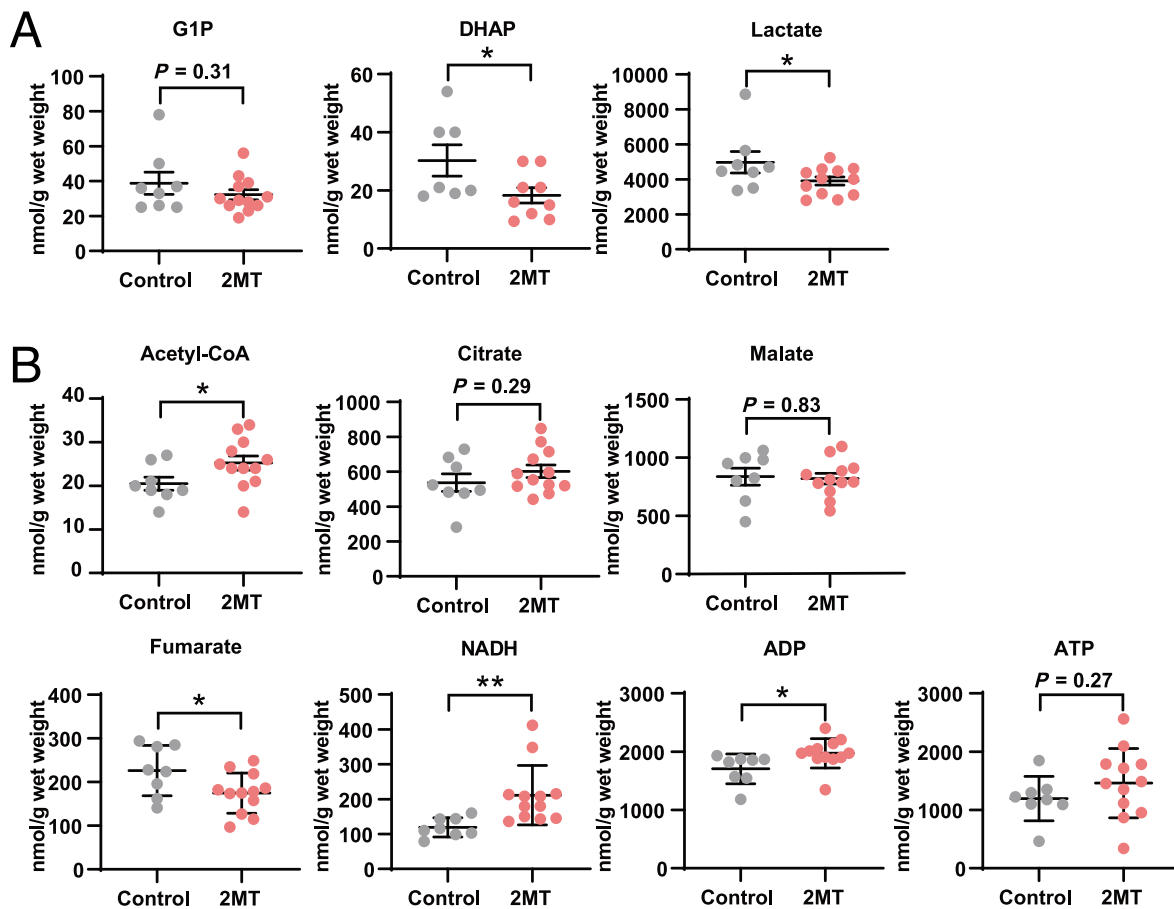
confirmed TRPA1 expression in those cells (*Figure S10*). ECAR and OCR were down-regulated following 2MT treatment depending on the concentration (*Figure 6D*). Thus, 2MT inhibited glycolysis and mitochondrial respiration with the core temperature decline in mice.

To further investigate the profiling change of the fuel in H9C2 cells following 2MT treatment, we performed glycolysis stress test. Unexpectedly, glycolysis was up-regulated following 2MT administration (*Figure S11*). Next, we performed palmitate oxidation stress test. Palmitate did not influence OCR level (*Figure S12A*), suggesting that the fuel dependence on fatty acid was low in H9C2 cells although the mammalian adult heart depends on fatty acid metabolism. However, endogenous fatty acid-dependent ATP production was reduced in the presence of 2MT (*Figure S12B*). These *in vitro* findings were not consistent with *in vivo* blood glucose increase and down-regulation of glycolysis-related metabolites in the metabolome analysis.

Discussion

We revealed the protective effect of subcutaneously administered 2MT in the I/R-injured mouse heart through hypothermia and metabolic energy modulation. 2MT administration before reperfusion reduced I/R-induced oxidative stress along with hypothermia and hypometabolism, resulting in a reduced infarct size and preserved left ventricle contractility. These results suggest a potential clinical application for 2MT in hypothermia therapy as an adjunct to PCI in patients with STEMI (*Figure 7*).

The metabolomic and intracellular influx analyses showed that metabolites of the TCA cycle, oxidative phosphorylation, and glycolysis were disturbed in the mouse heart following 2MT administration. The cardioprotective effect of hypothermia therapy is partly attributed to the metabolic changes caused by lowered body temperature.[31] Glucose metabolism is modulated following both insulin resistance and glucose

Figure 6 2MT modulates glucose metabolism and mitochondrial respiration. (A) Blood glucose concentration after a subcutaneous injection of 2MT (50 mg/kg) or saline (left graph) and changes (right graph) 30 min after injection ($n = 5$ for each group). (B) Serum insulin levels (left graph) ($n = 5$ for each group) and glucagon levels (right graph) (control $n = 4$, 2MT $n = 5$) 1 h after a subcutaneous injection of 2MT (50 mg/kg) or saline. (C) BAT activity was detected by PET/CT image after a subcutaneous injection of 2MT (50 mg/kg) or saline (left) and quantification of SUV (right) (control $n = 8$, 2MT $n = 6$). (D) Representative plot of ECAR (left graph) and OCR (right graph) measured in H9C2 cells following treatment with 2MT (0, 0.1 or 1 mM) ($n = 10$ for each group). Sequential addition of oligomycin (Oligo), FCCP (carbonyl cyanide p-trifluoromethoxyphenylhydrazone), and rotenone/antimycin A (R/A) is indicated in the graph. *$P < 0.05$, **$P < 0.01$; two-tailed Student t test. All values are mean ± standard deviation (SD). Each dot represents one mouse. 2MT, 2-methyl-2-thiazoline; BAT, brown adipose tissue; PET/CT, positron emission tomography/computed tomography; SUV, standardized uptake value; ECAR, extracellular acidification rate; OCR, oxygen consumption rate.
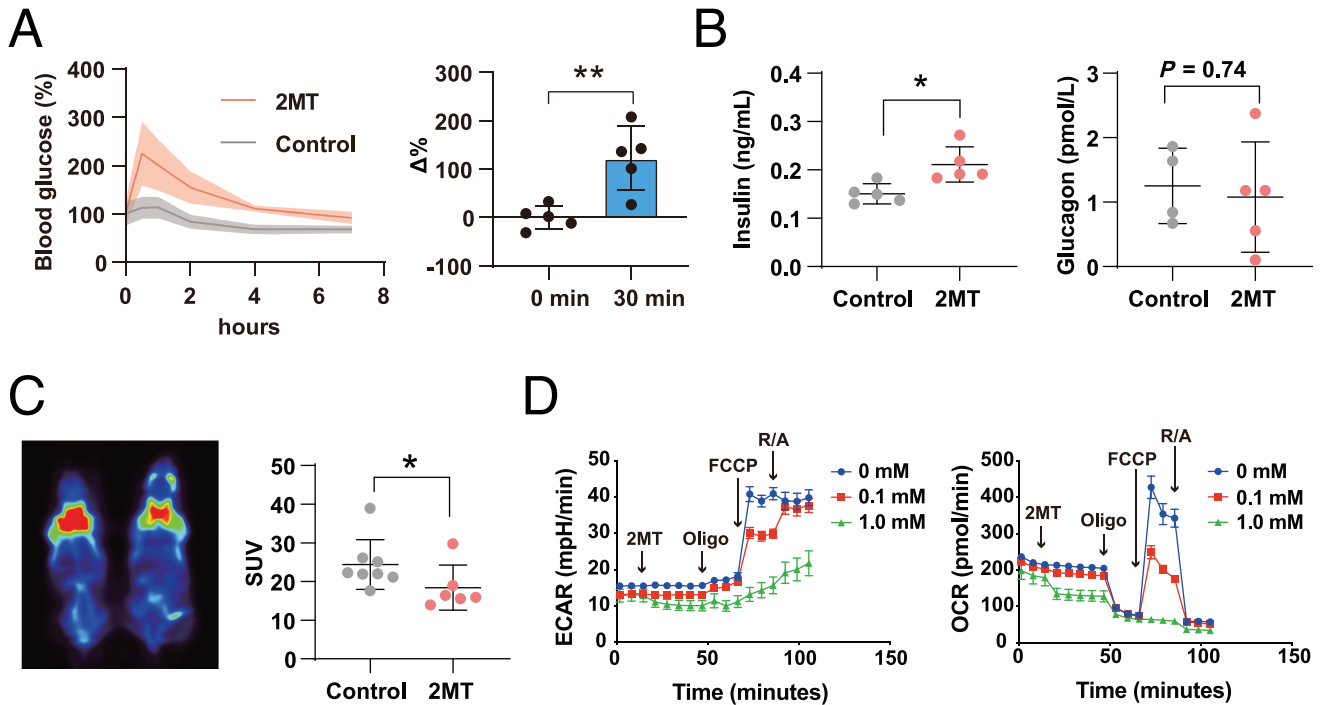
uptake, and BAT is responsible for converting the energy generated by metabolism into heat in mammals. 2MT administration promoted an increase in insulin resistance and a decrease in glucose uptake, resulting in increased blood glucose levels. The BAT activity was lower in 2MT-administered mice following cold exposure at 4°C, consistent with the

Figure 7 The schematic diagram showing the working hypothesis. Pre-administration of 2MT reduces oxidative stress in ischaemia/reperfusion area via the suppression of mitochondrial respiration and glycolysis, resulting in cardioprotection with mild hypothermia at coronary intervention.
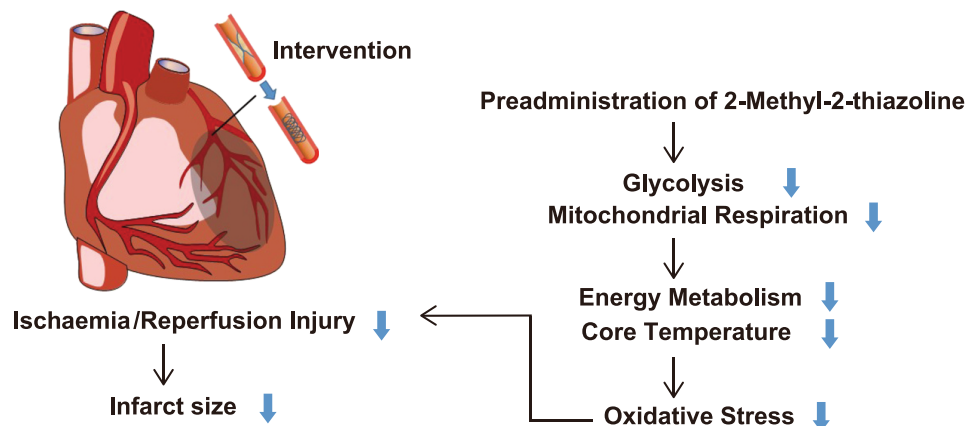
blood glucose levels in mice. 2MT also tended to preserve the adenylate energy charge in the hearts. This trend may indicate that 2MT is useful in cardiac energy saving under I/R injury through keeping cardiac adenosine stores. However, it is possible that other mechanisms unrelated to energy metabolism, such as changes in the thermal set-point at the temperature centre, are involved in the temperature decrease, and further studies are needed to elaborate on the mechanism of temperature decrease by 2MT.

This hypometabolic state induced by 2MT is similar to hibernation and torpor characterized by a temporary reduction in body temperature and energy expenditure. Hibernating mammals survive a low food supply by inducing a hypometabolic state.[32] Numerous cellular processes are halted during hibernation, including transcription, translation, and ion homeostasis. Subsequently, these alterations conserve energy sources, prevent cell death, and limit organ injury.[33] Recent reports have shown that a hypothalamic neuronal circuit induces a hibernation-like state, even in mice that are not hibernating.[34,35] Although it remains unknown whether 2MT mimics the hibernation state, 2MT administration simultaneously caused hypothermia and hypometabolism in non-hibernating animals, including mice. Hence, we speculate that 2MT may become a candidate compound for hypothermia therapy in non-hibernating mammals.

In the present study, we revealed that subcutaneous 2MT administration ameliorated I/R injury in the heart and suppressed mitochondrial respiration in cardiomyoblasts. 2MT-administered mice showed relatively reduced succinate and mitochondrial respiration, contributing to ROS reduction. Succinate enhances ROS production via mitochondrial electron transmission in the ischaemic heart.[6,7] 2MT reduced endogenous fatty acid-dependent ATP production in rat cardiomyoblasts H9C2 cells, suggesting that 2MT suppresses ROS production in the adult heart, which depends on fatty acid metabolism. However, the *in vitro* findings of glycolysis stress test using H9C2 cells were not consistent with *in vivo* blood glucose increase and down-regulation of glycolysis-related metabolites by 2MT. These metabolites are instantaneous. Mitochondria have a system of mitochondrial shuttles to transport reduced equivalents across the mitochondrial inner membrane, and various metabolites may be transferred to subsequent metabolism. Furthermore, given that the fuel dependence on fatty acid was low in H9C2 cells, these *in vitro* opposite findings need to be considered as a study limitation.

Metabolome analysis showed an increase in NADH in cardiac tissue with 2MT. NADH is related to mitochondrial ROS. Increased NADH with 2MT treatment can contribute to increased ROS generation. However, in the heart after I/R injury, 2MT had a significant decrease in tissue ROS and reduced, although not significantly, intracellular and mitochondrial ROS generation. It is difficult to fully explain our results

regarding ROS with NADH alone. In addition to the electron transport chain of mitochondria including NADH, other mechanisms, such as nitric oxide synthase and arachidonic acid oxidation, can also cause ROS generation that may contribute to I/R injury.[36] Further detailed research is needed to answer this question.

Previous data strongly suggest an association with 2MT and TRPA1, but the role of TRPA1 during ischaemic damage has not been well established. Although our previous reports indicate that in trigeminal/vagus nerves TRPA1 acts as a chemosensor and affects systemic energy metabolism via peripheral sensory nerves,[37] the present data suggest that 2MT may have a direct effect on cardiomyocytes. TRPA1 deficiency reportedly ameliorates myocardial I/R injury and mediates enhanced Ca^{2+} levels in cardiomyocytes.[38,39] Furthermore, TRPA1 is known to activate the protein kinase B (Akt)/endothelial NOS pathway in cardiomyocytes, resulting in attenuation of ischaemia-induced cardiomyocyte cell death.[40] These reports suggest that TRPA1 may be directly involved in the effect of subcutaneous 2MT administration on cardiomyocytes, resulting in a cardioprotective effect. Further studies are needed to elucidate the detailed systemic and cardiac protective effects of 2MT involving the role of TRPA1 in cellular oxidative stress.

The cardioprotective effect of 2MT remains to be further investigated for the translation to clinical practice. The present study revealed the cardioprotective effect with mild hypothermia induced by subcutaneous 2MT administration, but the impact of 2MT on non-rodent animals or human remains unclear. The genotoxicity of 2MT for human is also controversial.[41] Even if 2MT itself is not available, other thiazoline compounds may have similar effects. In fact, some thiazoline analogues other than 2MT induce hypothermia and hypoxia resistance.[37] Furthermore, human and mouse TRPA1 differ in ligand responsiveness.[42] To establish the cardioprotective effect of 2MT or similar thiazoline compounds in human, it is necessary to evaluate the effect of 2MT or similar thiazoline compounds in large mammals by comparing the drug-treated group with the conventional hypothermic group. In the future, it may be possible to identify other non-toxic thiazoline compounds with similar effects and use them in clinical practice.

In conclusion, we revealed the cardioprotective effect of 2MT on I/R injury by sparing energy metabolism with reversible hypothermia. To date, an effective treatment strategy for I/R injury during MI has not been established. Although further study is needed to clarify the mechanism and biological effects of 2MT before clinical applications, the present investigation has demonstrated sufficient impact to propose novel therapeutic approaches for the prevention of reperfusion injury during MI treatment. We believe that the concept of optimizing cellular metabolism through drug-induced hypothermia therapy is extremely useful in considering new therapeutic strategies for ischaemic heart disease.

Conflict of interest

None.

Funding

Supporting information

Additional supporting information may be found online in the Supporting Information section at the end of the article.

Data S1. Supporting Information.

Figure Sl. Evaluation of ROS production in mouse hearts and H9C2 cells following 2MT administration. (A) DHE staining was performed to evaluate ROS production in mouse hearts following 1/R injury (n = 6 for each group).*$P < 0.05$, **$P < 0.01$; one-way ANOVA with Tukey post hoc test for multiple group analysis. All values are mean± standard deviation (SD). H9C2 cells were incubated with 10 M CM-H2DCFDAdye or 5 J.LM MitoSOX for 60 min at 37°C to measure ROS generation (B) and mitochondrial superoxide (C) (n = 6 for each group). Cells were pretreated with 0.1 mM 2MT for 30 min and were then treated with 300 μM H_2O_2 for 3 hours. 1/R, ischemia–reperfusion; 2MT, 2-methyl-2-thiazoline; ROS, reactive oxygen species.

Figure S2. Cardiae function and remodelling 3 weeks after ischemialreperfusion injury. (A) Echocardiographic findings 3 weeks after IRI. n = 8 per group. (B) Masson's trichrome staining and fibrosis analysis of the myocardium 3 weeks after IRI.n = 8 and 7 insaline and 2MT-treated group respectively. Scale bar is 1 mm.**$P < 0.01$ between indicated groups. All values are mean;i:standard deviation (SD). 2MT, 2-methy1–2- thiazoline; Dd, left ventricular internal dimension in diastole; Ds, left ventricular diameter at end systole; FS, fractional shortening; EF, ejection fraction; IRI, ischemia/reperfusion injury.

Figure S3. PC-corr network between genes obtained from microarray analysis. The network is constructed according to the loading of PCl at a cut-off of0.7. Red nodes indicate genes with higher expression in 2MT-administered mouse hearts, while grey nodes indicate genes with higher expression in control mouse hearts. Node size is proportional to the node degree. The colour of interaction denotes the direction of the Pearson correlation between the features: red for positive Pearson correlation and bllack for negative case. The abbreviations are the official gene symbol.

Figure S4. Volcano plot of microarray data of mice heart. 2MT (50 mglkg) or saline was subcutaneously injected to the mice. Hearts were analysed 4 h after injection. The horizontal dashed line indicates the threshold at P-value = 0.01.

Figure S5. Microarray analysis for 1/R-injured mouse hearts. (A) Principal component analysis of microarray data (n = 3 for each group). Red nodes indicate 2MT; black nodes indicate control. (B) Enrichment analysis conducted by DAVID. The top 10 GO pathways are ranked by Benjamini-adjusted P values and scaled according to the function -log $_1$ (P-value). I/R, ischemia–reperfusion; 2MT, 2-methyl-2-thiazoline; PCl, first principal component; PC2, second principal component.

Figure S6. Core temperature of mouse following subcutaneous administration of lMT (100 mglkg).

Figure S7. Adenylate energy charge in the cardiac tissue. Adenylate energy charge was calculated from the formula (ATP + 0.5 * ADP)/(ATP + ADP + AMP). Data are presented as mean value ± SD (nmol/g wet weight).

Figure S8. Intracellular flux analysis after i.p injection of 13C glucose in 2MT or saline-administered mouse heart. White filled circles indicates 12C, black filled circle indicates 13C.

Figure S9. Cell viability of H9C2 cells against 2MT. Representative photos (A) and quantitative data (B) at 2 hours post-stimulation. Scale bar is 500 μm **$P < 0.01$; one-way ANOVA was done with Tukey post hoc test for multiple group analysis.

Figure S10. TRPAl expression in cardiomyocytes and H9C2 cells. HEK293T cells and myofibroblasts are negative and positive controls, respectively. Primary cardiomyocytes and myofibroblasts were isolated from the heart of neonatal Wistar rats. CMC, cardiomyocytes; 293 T, HEK293T cells; MFB, myofibroblasts.

Figure S11. Glycolysis stress test in H9Cl cells. Representative plot of ECAR measured in H9C2 cells following sequential addition of2MT (0, 0.1 or 1 mM), glucose, oligomycin, and 2-DG. n = 10 for each group. All values are mean±standard deviation (SD). ECAR, extracellular acidification rate; 2-DG, 2-deoxy-D-glucose.

Figure S12. Fatty acid-dependent ATP production in H9C2 cells. Reduction level of oxygen consumption rate by oligomycin in the presence ofBSA or palrnitate-BSA (A) and in the presence of BSA or BSA with etomoxir (B). All values are rnean±standard deviation (SD). OCR, oxygen consumption rate; BSA, bovine serum albumin; Eto, etornoxir.

References

1. Benjamin EJ, Virani SS, Callaway CW, Chamberlain AM, Chang AR, Cheng S, Chiuve SE, Cushman M, Delling FN, Deo R, de Ferranti SD, Ferguson JF, Fornage M, Gillespie C, Isasi CR, Jimenez MC, Jordan LC, Judd SE, Lackland D, Lichtman JH, Lisabeth L, Liu S, Longenecker CT, Lutsey PL, Mackey JS, Matchar DB, Matsushita K, Mussolino ME, Nasir K, O'Flaherty M, Palaniappan LP, Pandey A, Pandey DK, Reeves MJ, Ritchey MD, Rodriguez CJ, Roth GA, Rosamond WD, Sampson UKA, Satou GM, Shah SH, Spartano NL, Tirschwell DL, Tsao CW, Voeks JH, Willey JZ, Wilkins JT, Wu JH, Alger HM, Wong SS, Muntner P, American Heart Association Council on Epidemiology and Prevention Statistics Committee and Stroke Statistics. Heart disease and stroke Statistics-2018 update: a report from the American Heart Association. *Circulation* 2018; **137**: e67–e492.

2. De Luca G, Suryapranata H, Stone GW, Antoniucci D, Tcheng JE, Neumann FJ, Van de Werf F, Antman EM, Topol EJ. Abciximab as adjunctive therapy to reperfusion in acute ST-segment elevation myocardial infarction: a meta-analysis of randomized trials. *JAMA* 2005; **293**: 1759–1765.

3. Keeley EC, Boura JA, Grines CL. Primary angioplasty versus intravenous thrombolytic therapy for acute myocardial infarction: a quantitative review of 23 randomised trials. *Lancet* 2003; **361**: 13–20.

4. Takii T, Yasuda S, Takahashi J, Ito K, Shiba N, Shirato K, Shimokawa H, Investigators M-AS. Trends in acute myocardial infarction incidence and mortality over 30 years in Japan: report from the MIYAGI-AMI registry study. *Circ J* 2010; **74**: 93–100.

5. Fox KA, Carruthers KF, Dunbar DR, Graham C, Manning JR, De Raedt H, Buysschaert I, Lambrechts D, Van de Werf F. Underestimated and underrecognized: the late consequences of acute coronary syndrome (GRACE UK-Belgian study). *Eur Heart J* 2010; **31**: 2755–2764.

6. Chouchani ET, Pell VR, Gaude E, Aksentijevic D, Sundier SY, Robb EL, Logan A, Nadtochiy SM, Ord ENJ, Smith AC, Eyassu F, Shirley R, Hu CH, Dare AJ, James AM, Rogatti S, Hartley RC, Eaton S, Costa ASH, Brookes PS, Davidson SM, Duchen MR, Saeb-Parsy K, Shattock MJ, Robinson AJ, Work LM, Frezza C, Krieg T, Murphy MP. Ischaemic accumulation of succinate controls reperfusion injury through mitochondrial ROS. *Nature* 2014; **515**: 431–435.

7. Kohlhauer M, Dawkins S, Costa ASH, Lee R, Young T, Pell VR, Choudhury RP, Banning AP, Kharbanda RK, Oxford Acute Myocardial Infarction S, Saeb-Parsy K, Murphy MP, Frezza C, Krieg T, Channon KM. Metabolomic profiling in acute ST-segment-elevation myocardial infarction identifies succinate as an early marker of human ischemia-reperfusion injury. *J Am Heart Assoc* 2018; **7**: e007546.

8. Hausenloy DJ, Yellon DM. Myocardial ischemia-reperfusion injury: a neglected therapeutic target. *J Clin Invest* 2013; **123**: 92–100.

9. Dash R, Mitsutake Y, Pyun WB, Dawoud F, Lyons J, Tachibana A, Yahagi K, Matsuura Y, Kolodgie FD, Virmani R, McConnell MV, Illindala U, Ikeno F, Yeung A. Dose-dependent cardioprotection of moderate (32℃) versus mild (35℃) therapeutic hypothermia in porcine acute myocardial infarction. *JACC Cardiovasc Interv* 2018; **11**: 195–205.

10. Knoop B, Naguib D, Dannenberg L, Helten C, Zako S, Jung C, Levkau B, Grandoch M, Kelm M, Zeus T, Polzin A. Cardioprotection by very mild hypothermia in mice. *Cardiovasc Diagn Ther* 2019; **9**: 64–67.

11. Erlinge D, Gotberg M, Lang I, Holzer M, Noc M, Clemmensen P, Jensen U, Metzler B, James S, Botker HE, Omerovic E, Engblom H, Carlsson M, Arheden H, Ostlund O, Wallentin L, Harnek J, Olivecrona GK. Rapid endovascular catheter core cooling combined with cold saline as an adjunct to percutaneous coronary intervention for the treatment of acute myocardial infarction. The CHILL-MI trial: a randomized controlled study of the use of central venous catheter core cooling combined with cold saline as an adjunct to percutaneous coronary intervention for the treatment of acute myocardial infarction. *J Am Coll Cardiol* 2014; **63**: 1857–1865.

12. Gotberg M, Olivecrona GK, Koul S, Carlsson M, Engblom H, Ugander M, van der Pals J, Algotsson L, Arheden H, Erlinge D. A pilot study of rapid cooling by cold saline and endovascular cooling before reperfusion in patients with ST-elevation myocardial infarction. *Circ Cardiovasc Interv* 2010; **3**: 400–407.

13. Gong P, Li CS, Hua R, Zhao H, Tang ZR, Mei X, Zhang MY, Cui J. Mild hypothermia attenuates mitochondrial oxidative stress by protecting respiratory enzymes and upregulating MnSOD in a pig model of cardiac arrest. *PLoS ONE* 2012; **7**: e35313.

14. Hypothermia after Cardiac Arrest Study G. Mild therapeutic hypothermia to improve the neurologic outcome after cardiac arrest. *N Engl J Med* 2002; **346**: 549–556.

15. Nichol G, Strickland W, Shavelle D, Maehara A, Ben-Yehuda O, Genereux P, Dressler O, Parvataneni R, Nichols M, McPherson J, Barbeau G, Laddu A, Elrod JA, Tully GW, Ivanhoe R, Stone GW, Investigators V. Prospective, multicenter, randomized, controlled pilot trial of peritoneal hypothermia in patients with ST-segment- elevation myocardial infarction. *Circ Cardiovasc Interv* 2015; **8**: e001965.

16. Testori C, Beitzke D, Mangold A, Sterz F, Loewe C, Weiser C, Scherz T, Herkner H, Lang I. Out-of-hospital initiation of hypothermia in ST-segment elevation myocardial infarction: a randomised trial. *Heart* 2019; **105**: 531–537.

17. Lang PJ, Davis M, Öhman A. Fear and anxiety: animal models and human cognitive psychophysiology. *J Affect Disord* 2000; **61**: 137–159.

18. LeDoux J. Rethinking the emotional brain. *Neuron* 2012; **73**: 653–676.

19. Ledoux JE, Muller J. Emotional memory and psychopathology. *Philos Trans R Soc Lond B Biol Sci* 1997; **352**: 1719–1726.

20. Isosaka T, Matsuo T, Yamaguchi T, Funabiki K, Nakanishi S, Kobayakawa R, Kobayakawa K. Htr2a-expressing cells in the central amygdala control the hierarchy between innate and learned fear. *Cell* 2015; **163**: 1153–1164.

21. Wang Y, Cao L, Lee CY, Matsuo T, Wu K, Asher G, Tang L, Saitoh T, Russell J, Klewe-Nebenius D, Wang L, Soya S, Hasegawa E, Cherasse Y, Zhou J, Li Y, Wang T, Zhan X, Miyoshi C, Irukayama Y, Cao J, Meeks JP, Gautron L, Wang Z, Sakurai K, Funato H, Sakurai T, Yanagisawa M, Nagase H, Kobayakawa R, Kobayakawa K, Beutler B, Liu Q. Large-scale forward genetics screening identifies Trpa1 as a chemosensor for predator odor-evoked innate fear behaviors. *Nat Commun* 2018; **9**: 2041.

22. Matsuo T, Isosaka T, Tang L, Soga T, Kobayakawa R, Kobayakawa K. Artificial hibernation/life-protective state induced by thiazoline-related innate fear odors. *Commun Biol* 2021; **4**: 101.

23. Nishi M, Ogata T, Cannistraci CV, Ciucci S, Nakanishi N, Higuchi Y, Sakamoto A, Tsuji Y, Mizushima K, Matoba S. Systems network genomic analysis reveals Cardioprotective effect of MURC/Cavin-4 deletion against ischemia/reperfusion injury. *J Am Heart Assoc* 2019; **8**: e012047.

24. Bohl S, Medway DJ, Schulz-Menger J, Schneider JE, Neubauer S, Lygate CA. Refined approach for quantification of in vivo ischemia-reperfusion injury in the mouse heart. *Am J Physiol Heart Circ Physiol* 2009; **297**: H2054–H2058.

25. R Core Team (2020). R: A language and environment for statistical computing. R Foundation for Statistical Computing, Vienna, Austria. https://www.R-project.org/

26. Berthiaume JM, Kurdys JG, Muntean DM, Rosca MG. Mitochondrial NAD

(+)/NADH redox state and diabetic cardiomyopathy. *Antioxid Redox Signal* 2019; **30**: 375–398.

27. Kobara M, Tatsumi T, Matoba S, Yamahara Y, Nakagawa C, Ohta B, Matsumoto T, Inoue D, Asayama J, Nakagawa M. Effect of ischemic preconditioning on mitochondrial oxidative phosphorylation and high energy phosphates in rat hearts. *J Mol Cell Cardiol* 1996; **28**: 417–428.

28. Tatsumi T, Matoba S, Kobara M, Keira N, Kawahara A, Tsuruyama K, Tanaka T, Katamura M, Nakagawa C, Ohta B, Yamahara Y, Asayama J, Nakagawa M. Energy metabolism after ischemic preconditioning in streptozotocin-induced diabetic rat hearts. *J Am Coll Cardiol* 1998; **31**: 707–715.

29. Ouellet V, Labbe SM, Blondin DP, Phoenix S, Guerin B, Haman F, Turcotte EE, Richard D, Carpentier AC. Brown adipose tissue oxidative metabolism contributes to energy expenditure during acute cold exposure in humans. *J Clin Invest* 2012; **122**: 545–552.

30. Virtanen KA, Lidell ME, Orava J, Heglind M, Westergren R, Niemi T, Taittonen M, Laine J, Savisto NJ, Enerback S, Nuutila P. Functional brown adipose tissue in healthy adults. *N Engl J Med* 2009; **360**: 1518–1525.

31. Tissier R, Chenoune M, Ghaleh B, Cohen MV, Downey JM, Berdeaux A. The small chill: mild hypothermia for cardioprotection? *Cardiovasc Res* 2010; **88**: 406–414.

32. Geiser F. Hibernation. *Curr Biol* 2013; **23**: R188–R193.

33. Bouma HR, Verhaag EM, Otis JP, Heldmaier G, Swoap SJ, Strijkstra AM, Henning RH, Carey HV. Induction of torpor: mimicking natural metabolic suppression for biomedical applications. *J Cell Physiol* 2012; **227**: 1285–1290.

34. Hrvatin S, Sun S, Wilcox OF, Yao H, Lavin-Peter AJ, Cicconet M, Assad EG, Palmer ME, Aronson S, Banks AS, Griffith EC, Greenberg ME. Neurons that regulate mouse torpor. *Nature* 2020; **583**: 115–121.

35. Takahashi TM, Sunagawa GA, Soya S, Abe M, Sakurai K, Ishikawa K, Yanagisawa M, Hama H, Hasegawa E, Miyawaki A, Sakimura K, Takahashi M, Sakurai T. A discrete neuronal circuit induces a hibernation-like state in rodents. *Nature* 2020; **583**: 109–114.

36. Zhao M, Zhu P, Fujino M, Zhuang J, Guo H, Sheikh I, Zhao L, Li XK. Oxidative stress in hypoxic-ischemic encephalopathy: molecular mechanisms and therapeutic strategies. *Int J Mol Sci* 2016; **17**: 2078.

37. Matsuo T, Isosaka T, Hayashi Y, Tang L, Doi A, Yasuda A, Hayashi M, Lee CY, Cao L, Kutsuna N, Matsunaga S, Matsuda T, Yao I, Setou M, Kanagawa D, Higasa K, Ikawa M, Liu Q, Kobayakawa R, Kobayakawa K. Thiazoline-related innate fear stimuli orchestrate hypothermia and anti-hypoxia via sensory TRPA1 activation. *Nat Commun* 2021; **12**: 2074.

38. Conklin DJ, Guo Y, Nystoriak MA, Jagatheesan G, Obal D, Kilfoil PJ, Hoetker JD, Guo L, Bolli R, Bhatnagar A. TRPA1 channel contributes to myocardial ischemia-reperfusion injury. *Am J Physiol Heart Circ Physiol* 2019; **316**: H889–H899.

39. Lu Y, Piplani H, McAllister SL, Hurt CM, Gross ER. Transient receptor potential Ankyrin 1 activation within the cardiac myocyte limits ischemia-reperfusion injury in rodents. *Anesthesiology* 2016; **125**: 1171–1180.

40. Andrei SR, Ghosh M, Sinharoy P, Damron DS. Stimulation of TRPA1 attenuates ischemia-induced cardiomyocyte cell death through an eNOS-mediated mechanism. *Channels (Austin)* 2019; **13**: 192–206.

41. Barbaro B, Baldin R, Kovarich S, Pavan M, Fioravanzo E, Bassan A. Further development and update of EFSA's Chemical Hazards Database. *EFSA Support Publ* 2015; **12**: EN-823.

42. Sinica V, Zimova L, Barvikova K, Macikova L, Barvik I, Vlachova V. Human and mouse TRPA1 are heat and cold sensors differentially tuned by voltage. *Cell* 2019; **9**: 57.